

A ${}^6\text{Li}$ – ${}^{13}\text{C}$ REDOR Study of the TMEDA Complex of Solid Fluorenyllithium

Per-Ola Quist,[§] Hans Förster,[‡] and Dan Johnels^{*,†}

Contribution from the Departments of Physical Chemistry and Organic Chemistry, Umeå University, S-901 87 Umeå, Sweden, and Bruker Analytische Messtechnik, D-76287 Rheinstetten, Germany

Received October 28, 1996[⊗]

Abstract: The solid-state structure of the TMEDA complex of fluorenyllithium is investigated by the ${}^6\text{Li}$ – ${}^{13}\text{C}$ REDOR NMR experiment. The REDOR experiment was performed on ${}^6\text{Li}$ -enriched samples with detection of the natural abundance ${}^{13}\text{C}$ -signal. This simplifies the interpretation of the data and also the sample preparation. The dipole–dipole couplings between the ${}^6\text{Li}$ cation and the ${}^{13}\text{C}$ nuclei, determined with the REDOR sequence, yields direct structural information. The distance information is also helpful when assigning the solid-state ${}^{13}\text{C}$ NMR spectrum. The position of the Li cation is determined to within ± 0.2 Å (with respect to the fluorenyl framework).

Introduction

The structure and reactivity of organolithium compounds are of fundamental interest to organic chemists, since they are widely used as reagents in organic synthesis. Accordingly, the structures of a great number of organolithium compounds have been studied in solution by different spectroscopic methods, mainly NMR spectroscopy,¹ and in the solid state by X-ray crystallography.² Organolithium compounds are often present as different types of ion pairs or aggregates both in solution and in the solid state. It is known that the degree of aggregation and solvation influences the reactivity, stereo selectivity, etc. in solution.³ In order to use this kind of reagents in an optimal fashion it is important to understand the factors that govern, for instance, the aggregation.

In an ongoing project, we use solid-state NMR spectroscopy to relate X-ray and NMR data sources and to check whether solid-state structures of organolithium compounds, as determined by X-ray crystallography, are relevant models for structures in solution. We have studied both systems of localized as well as delocalized carbanions by solid state NMR spectroscopy.⁴ In a solid-state ${}^{13}\text{C}$ magic-angle spinning (MAS) NMR spectroscopic study of different fluorenyllithium complexes, we showed that the structures of the complexes were dependent on the type of ligand used.^{4a} In the bis-quinuclidine complex the lithium

cation was found to be asymmetrically positioned relative to the fluorenyl framework, in accordance with the earlier reported X-ray structure.⁵ The same is true for the diethyl ether (DEE) complex.^{4a} However, in the N,N,N',N' -tetramethylethylenediamine (TMEDA) complex the system is symmetric according to the ${}^{13}\text{C}$ solid-state NMR spectrum.^{4a} The THF coordinated system shows a symmetric structure as well.^{4a}

In another report we investigated the fluorenyllithium complexes by solid-state ${}^7\text{Li}$ NMR spectroscopy under MAS and static conditions.^{4d} The results further supported a symmetric TMEDA complex. In the MAS studies the chemical shift show the expected dependence of the position of the lithium cation relative to the fluorenyl system. The chemical shift is about -7 ppm if the lithium cation resides above the carbanion framework and about -2 ppm otherwise. The quadrupolar coupling constant is also sensitive to changes in the cation position. In this context, it is important to note that all experimental data acquired so far are consistent with a lithium cation located above the five-membered ring in the TMEDA complex of fluorenyllithium. The results from these studies are also in accordance with the proposal that the energy surface is rather shallow for delocalized carbanions⁶ and that other factors, such as the steric demand of the ligand or crystal packing forces, may determine the actual crystal structure. Although these experimental and theoretical studies support a symmetric complex, a more definite experimental investigation should be performed before the problem is settled. This is the intention of the present work where we determine the dipole–dipole coupling and thus the distance between the ${}^6\text{Li}$ cation and the ${}^{13}\text{C}$ nuclei in the fluorenyl framework. In solution, a lithium–carbon and lithium–proton HOESY study was recently used to obtain information on the position of the lithium ion in a benzyllithium compound.^{1e}

The development of solid-state NMR methods during the last decade has been extremely fast. Methods for the determination of internuclear distances based on the dipole–dipole coupling was proposed at the end of the last decade.^{7,8} One of these methods, the Rotational-Echo, Double-Resonance (REDOR) experiment was initially designed to determine the heteronuclear

[†] Department of Organic Chemistry, Umeå University.

[‡] Bruker Analytische Messtechnik.

[§] Department of Physical Chemistry, Umeå University.

[⊗] Abstract published in *Advance ACS Abstracts*, May 15, 1997.

(1) (a) Günther, H.; Moskau, D.; Bast, P.; Schmalz, D. *Angew. Chem., Int. Ed. Engl.* **1987**, *26*, 1212. (b) Thomas, R. D. In *Isotopes in the Physical and Biomedical Science*; Buncel, E., Jones, J. R., Eds.; Elsevier: Amsterdam, 1991. (c) Bauer, W.; Schleyer, P. v. R. *Adv. Carbanion Chem.* **1992**, *1*, 89. (d) Bauer, W. In *Lithium Chemistry*; Sapse, A.-M., Schleyer, P. v. R., Eds.; Wiley-Interscience Publication: New York, 1995. (e) Berger, S.; Müller, F. *Chem. Ber.* **1995**, *128*, 799.

(2) (a) Setzer, W. N.; Schleyer, P. v. R. *Adv. Organomet. Chem.* **1985**, *24*, 353. (b) Seebach, D. *Angew. Chem., Int. Ed. Engl.* **1988**, *27*, 1624. (c) Weiss, E. *Angew. Chem., Int. Ed. Engl.* **1993**, *32*, 1501. (d) Boche, G.; Lohrenz, J. C. W.; Opel, A. In *Lithium Chemistry*; Sapse, A.-M., Schleyer, P. v. R., Eds.; Wiley-Interscience Publication: New York, 1995. (e) Pauer, F.; Power, P. In *Lithium Chemistry*; Sapse, A.-M., Schleyer, P. v. R., Eds.; Wiley-Interscience Publication: New York, 1995.

(3) (a) Juaristi, E.; Beck, A. K.; Hansen, J.; Matt, T.; Mukhopadhyay, T.; Simson, M.; Seebach, D. *Synthesis* **1993**, *12*, 1271. (b) Jackman, L. M.; Petrei, M. M.; Smith, B. D. *J. Am. Chem. Soc.* **1991**, *113*, 3451.

(4) (a) Johnels, D.; Edlund, U. *J. Am. Chem. Soc.* **1990**, *112*, 1647. (b) Johnels, D.; Edlund, U. *J. Organomet. Chem.* **1990**, *393*, C35. (c) Johnels, D. *J. Organomet. Chem.* **1993**, *445*, 1. (d) Johnels, D.; Andersson, A.; Boman, A.; Edlund, U. *Magn. Reson. Chem.* **1996**, *34*, 908.

(5) Brooks, J. J.; Rhine, W.; Stucky, G. D. *J. Am. Chem. Soc.* **1972**, *94*, 7339.

(6) Bushby, R. J.; Steel, H. L. *J. Chem. Soc., Perkin Trans. 2* **1990**, *27*, 1169.

(7) Raleigh, D. P.; Levitt, M. H.; Griffin, R. G. *Chem. Phys. Lett.* **1988**, *146*, 71.

dipole–dipole constant between two spin $S = I = 1/2$ nuclei.⁸ Recently, the method was extended to the investigation of a heteronuclear spin system with a spin $S = 1/2$ and a spin $I = 1$, i.e., ¹³C and ²H in DL-[2-²H,3-¹³C] alanine.⁹ For comprehensive reviews of these and similar methods, we recommend the reader to take part of some of the numerous reviews of the field.^{10–13}

In this work, we report the application of the REDOR experiment to determine the dipole–dipole coupling and thereby the distance between ¹³C ($S = 1/2$) and ⁶Li ($I = 1$) in an organolithium system. The system under study is the TMEDA complex of fluorenyllithium mentioned above. By using ⁶Li enriched material and natural abundance ¹³C the sample preparation is simplified since no ¹³C labeling is necessary. Furthermore, the interpretation of the REDOR decay simplifies since all ¹³C nuclei in the fluorenyl framework interact with the ⁶Li nuclei in the complex, hence several sources to possible systematic errors are avoided.¹⁴ As the acquisition is performed in a two-dimensional fashion, a single experiment determines the dipole–dipole coupling between all ¹³C and the ⁶Li. To deconvolute the REDOR decays from the superpositions in the ¹³C spectrum, we use a slightly revised form of the recently derived REDOR transform.¹⁵

Theory

The REDOR experiment developed by Schaefer and co-workers⁸ is designed to measure the heteronuclear dipole–dipole coupling between two nuclei under MAS conditions. The basics of the REDOR experiment is the application of rotor synchronized π -pulses (180°-pulses) on one of the nuclei, which inverts the sign of the heteronuclear dipole–dipole Hamiltonian in a systematic way. This prevents the dipole–dipole Hamiltonian from forming rotational echoes, that otherwise would occur every full rotor period.¹⁶ For detailed discussions of the REDOR experiment, see for instance refs 8 and 17.

In this investigation, we use the REDOR experiment to determine the distance between a ⁶Li cation ($I = 1$) and the ¹³C nuclei ($S = 1/2$) in the fluorenyl complex. We use the REDOR experiment described in a recent communication by Schmidt et al.⁹ Unfortunately, this work is flawed by some serious misprints.¹⁸ Therefore, we will derive some of the necessary expressions below.

After transformation to a doubly rotating frame, the relevant Hamiltonian for a two-spin system with $S = 1/2$ and $I = 1$ under MAS, is given by^{16,19}

$$\hat{H}(t) = \omega_Q(t)[3\hat{I}_z^2 - I(I+1)] + \omega_I(t)\hat{I}_z + \omega_S(t)\hat{S}_z + \omega_D(t)\hat{I}_z\hat{S}_z \quad (1)$$

It was shown by Schmidt et al.⁹ that after a complete rotor period, the net effect of the quadrupolar interaction (ω_Q), the

(8) (a) Gullion, T.; Schaefer, J. *Adv. Magn. Reson.* **1989**, *13*, 57. (b) Gullion, T.; Schaefer, J. *J. Magn. Reson.* **1989**, *81*, 196.

(9) Schmidt, A.; McKay, R. A.; Schaefer, J. *J. Magn. Reson.* **1992**, *96*, 644.

(10) Griffiths, J. M.; Griffin, R. G. *Anal. Chim. Acta* **1993**, *283*, 1081.

(11) Bennet, A. E.; Griffin, R. G.; Vega, S. In *NMR, Basic Principles and Progress*, Vol 33; Diehl, P., Fluck, E., Günther, H., Kosfeld, R., Seelig, J., Blümich, B., Eds.; Springer-Verlag: Berlin, 1994; pp 3–77.

(12) Opella, S. J. *Annu. Rev. Phys. Chem.* **1994**, *45*, 659.

(13) Hong, M.; Schmidt-Rohr, K.; Nanz, D. *Biophys. J.* **1995**, *69*, 1939.

(14) Naito, A.; Nishimura, K.; Kimura, S.; Tuzi, S.; Aida, M.; Yasuoka, N.; Saito, H. *J. Phys. Chem.* **1996**, *100*, 14995.

(15) (a) Mueller, K. T.; Jarvie, T. P.; Aurentz, D. J.; Roberts, B. W. *Chem. Phys. Lett.* **1995**, *242*, 535. (b) Mueller, K. T.; Jarvie, T. P.; Aurentz, D. J.; Roberts, B. W. *Chem. Phys. Lett.* **1996**, *254*, 281.

(16) Maricq, M. M.; Waugh, J. S. *J. Chem. Phys.* **1979**, *70*, 3300.

(17) Mueller, K. T. *J. Magn. Reson. A* **1995**, *113*, 81.

(18) Schaefer, J. Personal communication.

chemical-shift interactions (ω_I and ω_S), and the dipole–dipole interaction (ω_D) is zero, which generates so-called rotational echoes at $t = nT_r$ (where $T_r = 2\pi/\omega_r$ is the rotor period) in the time-domain signal. At any other time rapid dephasing of the signal is expected. However, with a suitable set of rotor synchronized π -pulses on one of the two nuclei (⁶Li in our case), it is possible to counteract the refocussing of the dipole–dipole Hamiltonian at every completed rotor period, thus creating a dephasing that depends on the dipole–dipole coupling between the two nuclei.^{8,9}

Under MAS conditions, the dipolar transition frequencies (ω_D) for an ensemble of isolated heteronuclear I–S spin pairs fluctuates with time. For the $I = 1$ nuclei, the states of the S-spin with $m_S = \pm 1/2$ splits the signal from the I-spins into two counter rotating magnetizations of equal amplitude and with angular frequencies given by^{8,16,19}

$$\omega_D(\alpha, \beta, t) = \pm \frac{D}{2} [\sin^2(\beta) \cos(2\alpha + 2\omega_r t) - \sqrt{2} \sin(2\beta) \cos(\alpha + \omega_r t)] \quad (2)$$

For the $S = 1/2$ nuclei, on the other hand, the states of the I-spin with $m_I = 0, \pm 1$ split the S-signal into three magnetizations with equal intensity and with angular frequencies^{16,19}

$$\omega_D^\pm(\alpha, \beta, t) = \pm D [\sin^2(\beta) \cos(2\alpha + 2\omega_r t) - \sqrt{2} \sin(2\beta) \cos(\alpha + \omega_r t)] \quad (3a)$$

and

$$\omega_D^0(\alpha, \beta, t) = 0 \quad (3b)$$

In eqs 2 and 3, α is the azimuthal angle and β is the polar angle between the internuclear I–S vector and the MAS rotor axis. Usually, the sample is a powder sample, making it necessary to integrate over α and β . $\omega_r = 2\pi/T_r$ is the MAS angular frequency and D is the heteronuclear dipole–dipole coupling in rad/s given by^{19,20}

$$D = \frac{\mu_0 \gamma_I \gamma_S \hbar}{4\pi r_{IS}^3} \approx \frac{2\pi \cdot 122 \cdot 10^3 \gamma_I \gamma_S}{(r_{IS}/\text{Å})^3 \gamma_H \gamma_H} \quad (4)$$

where r_{IS} is the distance (in Å) between the I and S nuclei in the isolated pairs.

In the following we concentrate on the REDOR experiment in Figure 1a. Here, the two refocussing π -pulses on the $I = 1$ nucleus reintroduce the dipolar term in eq 1 but have no net effect on the other terms in the total Hamiltonian.⁹ The effect of each π -pulse on the heteronuclear dipole–dipole term is to invert the sign of the dipolar transition frequencies in eqs 2 and 3. If we assume that for each rotor period, the pair of π -pulses is applied symmetrically (cf. Figure 1a), i.e., at $(T_r - \tau)/2$ and $(T_r + \tau)/2$, the net phase, $\Delta\phi(\alpha, \beta, \tau)$, acquired by the S-spins at the angle (α, β) under one rotor period is given by

$$\Delta\phi^\pm(\alpha, \beta, \tau) = \int_0^{(T_r - \tau)/2} dt \omega_D(\alpha, \beta, t) - \int_{(T_r - \tau)/2}^{(T_r + \tau)/2} dt \omega_D(\alpha, \beta, t) + \int_{(T_r + \tau)/2}^{T_r} dt \omega_D(\alpha, \beta, t) = \mp \frac{2D}{\omega_r} \left[2\sqrt{2} \sin(2\beta) \cos(\alpha) \sin\left(\frac{\omega_r \tau}{2}\right) + \sin^2(\beta) \cos(2\alpha) \sin(\omega_r \tau) \right] \quad (5a)$$

(19) Schmidt-Rohr, K.; Spiess, H. W. *Multidimensional Solid-State NMR and Polymers*; Academic Press: London, 1994.

(20) Abragam, A. *The Principles of Nuclear Magnetism*; Clarendon Press: Oxford, 1961.

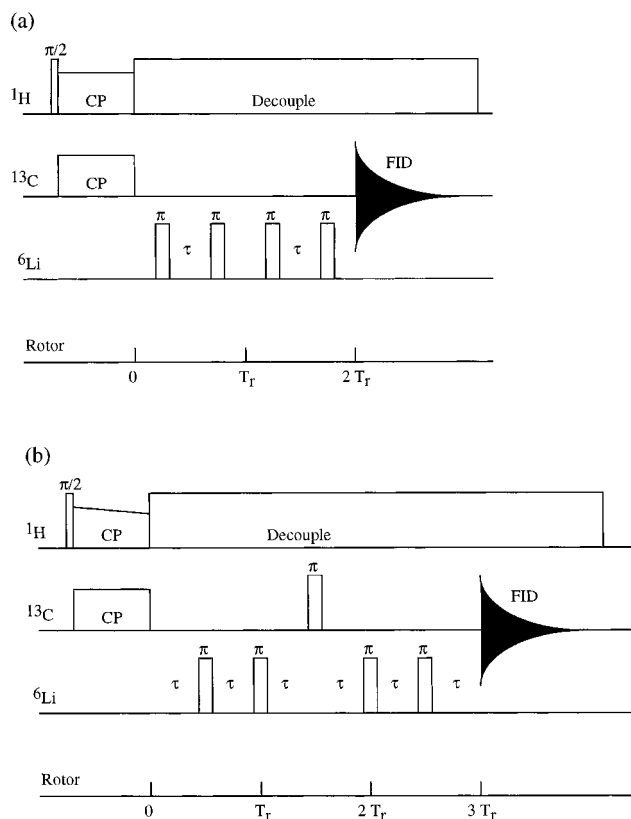


Figure 1. (a) The REDOR pulse sequence used to calculate the decay in eq 8. T_r is the rotor period, and τ is the spacing between the symmetrically applied pulses. (b) The pulse sequence used to determine the ${}^6\text{Li}$ – ${}^{13}\text{C}$ dipole–dipole couplings. This sequence is an expansion of the sequence in (a) by a symmetrically placed ${}^{13}\text{C}$ chemical-shift refocusing π -pulse. The acquisition of the ${}^{13}\text{C}$ signal dephasing was made with $\tau = T_r/2$ and $N_C = 0, 2, 4, 6, \dots$

and

$$\Delta\phi^0(\alpha, \beta, \tau) = 0 \quad (5b)$$

If we repeat the pair of refocussing π -pulses each rotor cycle (cf. Figure 1a, where we have two rotor periods), the dephasing of the S -signal increases linearly with the number of rotor periods with two refocussing π -pulses (N_C),⁸ which accumulates to a total phase of

$$\Delta\Phi(\alpha, \beta, \tau) = N_C \Delta\phi(\alpha, \beta, \tau) \quad (6)$$

For the special case of evenly spaced refocussing π -pulses, i.e., we set $\tau = T_r/2$, eqs 5 and 6 reduce to

$$\Delta\Phi^\pm(\alpha, \beta, T_r/2) = \mp \frac{2\sqrt{2}DN_C T_r}{\pi} \sin(2\beta) \cos(\alpha) \quad (7a)$$

and

$$\Delta\Phi^0(\alpha, \beta, T_r/2) = 0 \quad (7b)$$

which after integration over a powder distribution in α and β yields the following signal decay from the $S = 1/2$ spins

$$S(T_r/2, N_C) = S_0 e^{-N_C T_r/T_2} \left\{ \frac{1}{3} + \frac{2}{32\pi} \int_0^{2\pi} d\alpha \int_0^{\pi/2} d\beta \times \sin \beta \cos[|\Delta\Phi^\pm(\alpha, \beta, T_r/2)|] \right\} \quad (8)$$

where we have added an effective exponential relaxation time T_2 that represents the dephasing due to transverse spin relaxation.

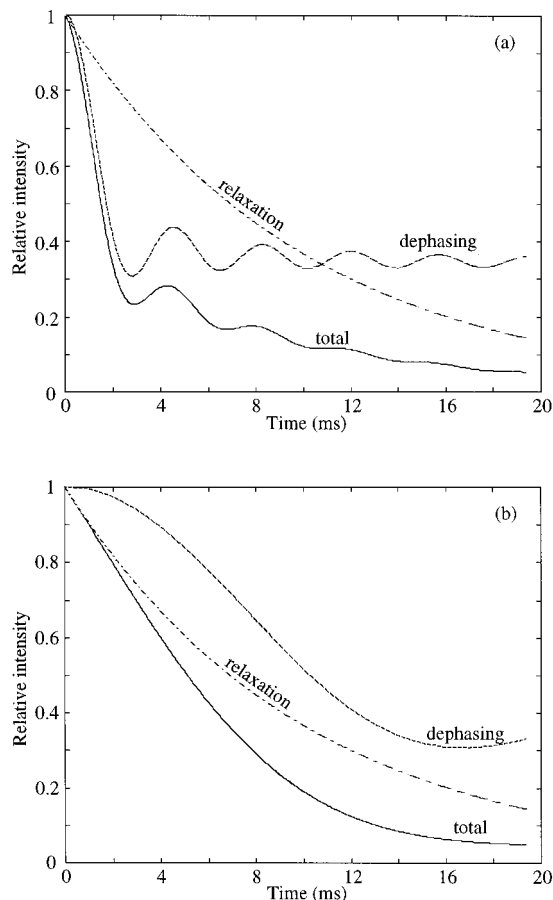


Figure 2. The expected shape of the intensity decay described by eq 8 assuming $T_2 = 10$ ms, $\omega_r = 2\pi \cdot 6200$ rad/s, $N_C = 0, 1, 2, \dots, 120$, and (a) $D = 2\pi \cdot 300$ rad/s or (b) $D = 2\pi \cdot 50$ rad/s. Solid lines: Decay of the observed signal. Dashed lines: The decay due to the REDOR induced dephasing. Dash-dot lines: The decay due to the transverse relaxation.

In Figure 1b, we have added a π -pulse on the ${}^{13}\text{C}$ ($S = 1/2$) and expanded the pulse sequence symmetrically around the two trains of refocussing π (${}^6\text{Li}$)-pulses. The net effect of this expansion is a refocussing of the isotropic ${}^{13}\text{C}$ chemical-shift variations in the sample, as described in the original papers by Gullion and Schaefer.⁸ This makes the sequence in Figure 1b more suitable for practical work. Fortunately, eq 8 is valid also for the expanded pulse sequence. This is because the π (${}^{13}\text{C}$)-pulse applied at the center of the experiment only refocus the dephasing of the ${}^{13}\text{C}$ magnetization due to magnetic field inhomogeneity and has no net effect on the dipolar term in the Hamiltonian.⁸ However, a comparison of Figure 1 (parts a and b) reveals that in the expanded pulse sequence, there is one rotor period without refocussing π (${}^6\text{Li}$)-pulses. In order to use eq 8 we should thus keep in mind that N_C is the number of rotor periods with refocussing π -pulses on the $I = 1$ nucleus and hence redefine the initial amplitude S_0 to include the small relaxation decay that occurs during the rotor period without π (${}^6\text{Li}$)-pulses. For a reference experiment *without* the refocussing π -pulses on the $I = 1$ spins in Figure 1b, eq 8 is still valid provided we replace the expression within the curly brackets by unity.

In Figure 2, we show the expected shape of eq 8 using two different values of the dipole–dipole coupling: 300 Hz (in Figure 2a) and 50 Hz (in Figure 2b). Notice that in the latter case the characteristic REDOR-induced undulations in the observed decay is hidden by the faster relaxation process.

There are thus two processes that contribute to the decay of the signal of the S -spins; the dephasing induced by the rotor synchronized π -pulses and the transverse relaxation. The first

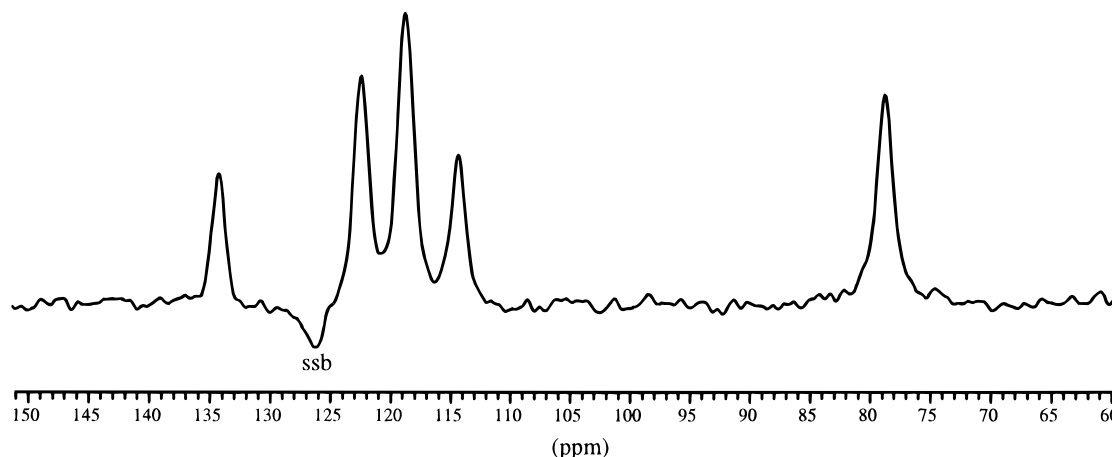


Figure 3. ^{13}C MAS spectrum of the TMEDA complex of solid fluorenyllithium. ssb = spinning sideband.

process is governed by the dipole–dipole coupling (D), the rotor period (T_r), and the number of rotor cycles before detection (N_C), while the second process is governed by the transverse relaxation time T_2 (assuming an exponential decay). In order to determine the dipole–dipole coupling accurately it is necessary that the REDOR induced dephasing dominates the observed decay, which implies that the observed decay must undulate. Furthermore, proper setting of the NMR spectrometer, the timing and phase cycling is also necessary due to the numerous π -pulses applied,²¹ that otherwise contributes with an additional dephasing of the signal.^{22,23}

To extend the range of the REDOR experiment, it is possible to determine the fraction of the decay due to the transverse relaxation by an additional experiment with no refocussing π -pulses on the $I = 1$ spins. However, one should keep in mind that in such an experiment the number of pulses is far fewer, making the spectrometer setting and timing extremely important. In the present work, this second experiment was made by repeating the REDOR sequence in Figure 1b, but now with the intensity of the π (^6Li)-pulses damped by 120 dB so that no excitation occurred. In order to obtain reliable results from the signals with decays dominated by transverse relaxation, one should ideally have a sample where the observed decay of at least one signal is dominated by the REDOR induced dephasing. If the two decays (with and without π (^6Li)-pulses) yield the same transverse relaxation time, this verifies a proper setting of the spectrometer. Fortunately, this is the case in the present investigation.

For the REDOR experiment with refocussing π -pulses on the $S = 1/2$ spins and stroboscopic sampling of the $I = 1$ signal, the acquired phase is half of that given by eqs 5a, 6, and 7a. In addition, there is only two counter rotating magnetizations. This yields a decay of the peaks of the $I = 1$ spins that is given by

$$I(T_r/2, N_C) = I_0 e^{-N_C T_r / T_2} \frac{1}{2\pi} \int_0^{2\pi} d\alpha \int_0^{\pi/2} d\beta \times \sin \beta \cos[|\Delta\Phi^\pm(\alpha, \beta, T_r/2)|/2] \quad (9)$$

which is identical to the REDOR decay from a heteronuclear pair both with spin $1/2$.⁸

The integral in eqs 8 and 9 can be solved either numerically or by the analytic solution derived by Mueller et al.¹⁵ In the latter case, the integral in eq 8 is given as the product of two

Bessel functions of the first kind

$$S(T_r/2, N_C) = S_0 e^{-N_C T_r / T_2} \left\{ \frac{1}{3} + \frac{2\sqrt{2}\pi}{3 \cdot 4} J_{1/4}(\sqrt{2}N_C D T_r / \pi) J_{-1/4}(\sqrt{2}N_C D T_r / \pi) \right\} \quad (10)$$

with our definitions. (For the more common case of two interacting spin $S = I = 1/2$ nuclei, the argument in eq 10 should be reduced by a factor of two, cf. eq 9). If the calculations are performed in an environment that cannot generate Bessel functions of the first kind with noninteger negative order, the following reflection formulas for Bessel functions can be used²⁴

$$J_{-p}(x) = \cos(p\pi)J_p(x) - \sin(p\pi)Y_p(x) \quad (11a)$$

$$Y_{-p}(x) = \sin(p\pi)J_p(x) + \cos(p\pi)Y_p(x) \quad (11b)$$

where $Y_p(x)$ is the Bessel function of the second kind and order p . If these Bessel functions cannot be generated, the problem can be settled by numerically solving the integral for about 1000 different input arguments (the product $DN_C T_r$), thus creating a table with the integral value as a function of $DN_C T_r$. This table can then be called by an interpolating look-up routine. A comparative calculation of the REDOR decay using eqs 8 and 10 yields a difference in the calculated signal that is less than 0.3%. Once the look-up table is created, the look-up procedure is about a factor of two faster in our calculation environment (MatLab 4.2 on a 150 MHz Power Macintosh). However, since 100 input arguments are returned in less than 1 s using eqs 10 and 11a, we use this method in the present work.

Results and Analysis

Spectral Analysis. As observed in Figure 3, the TMEDA complex of fluorenyllithium shows a solid-state ^{13}C NMR spectrum consisting of five signals from the fluorenyl framework, at 78, 114, 119, 122, and 134 ppm, respectively. It is important to notice that the 13 carbons in the fluorenyl system only give rise to five peaks. This implies that the TMEDA complex of fluorenyllithium is mirror symmetric, with respect to the plane $x = 0$ in Figure 4, and that two of the peaks are superpositions. The symmetry may be static or an effect of a dynamic process occurring on a time scale long compared to the inverse of the difference in carbon frequency for the various

(21) Cory, D. G.; Maas, W. E. J. R. *J. Magn. Reson. A* **1993**, *102*, 190.

(22) Gullion, T.; Baker, D. B.; Conradi, M. S. *J. Magn. Reson.* **1990**, *89*, 479.

(23) McDowell, L. M.; Holl, S. M.; Qian, S.; Li, E.; Schaefer, J. *Biochemistry* **1993**, *32*, 4560.

(24) Press, W. H.; Flannary, B. P.; Teukolsky, S. A.; Vetterling, W. T. *Numerical Recipes in Fortran*; Cambridge University Press: Cambridge, 1992.

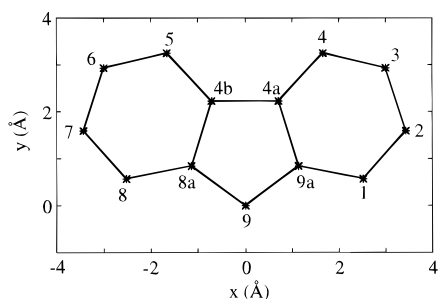


Figure 4. Structure of the anionic fluorenyl framework as derived from an X-ray study of fluorenylsodium.²⁹ Since the sodium cation is asymmetrically located with respect to the fluorenyl framework, this fluorenyl framework is not symmetric. To calculate the structure for fluorenyllithium we symmetrized the fluorenyl molecule, which changed the position of the carbons by less than 0.01 Å.

sites.²⁵ The frequency difference between some (real or hypothetical) sites can be estimated to be in the order of 1 kHz. Hence, if some motion occurs in the TMEDA complex of fluorenyllithium, the correlation times are probably faster than milliseconds. This is in agreement with an earlier variable temperature study, where no dynamics of the fluorenyl framework was detected in the range from 213 to 273 K.^{4a} In the TMEDA ligand, however, a dynamic process was observed to slow down in this temperature range.^{4a} The dynamics of the TMEDA ligand have been investigated in detail in some other organolithium complexes.²⁶ Since the present study was performed at ambient temperatures, the dynamics should be in the fast exchange regime. Whether this motional mode of the TMEDA ligand significantly affects the relative position of the Li cation to the fluorenyl system remains to be determined.

From a comparison with the ¹³C spectrum of the compound in solution²⁷ the peaks at 78, 114, and 134 ppm could be assigned to carbons 9, 3, and 9a, respectively (defined in Figure 4). Hence, there are three assigned signals for the determination of the position of the Li cation. This is sufficient to settle a unique structure—if the Li cation only occupies one site (cf. below).

According to the intensities in Figure 3, the peaks at 119 and 122 ppm are probably superpositions, from two different carbons, each. This is in accordance with the chemical shifts for carbons 1, 2, 4, and 4a, which are observed in this range.²⁷ In a recent publication¹⁵ a data processing routine was described that makes it possible to separate the REDOR decays from several superimposed peaks. The REDOR transform was defined as

$$\int_0^{\infty} S(D_i t) K(D_i t) F(t) dt = S_{i0} \delta(D - D_i) \quad (12a)$$

where S is the REDOR decay from the superposition with D_i representing different dipole–dipole couplings, K is the kernel of the transform, F is a filter used to damp the diverging kernel, and S_{i0} is the amplitude of the individual signals that overlap. In eq 12a, δ represents a delta function only when the filter function equals unity. In practice, δ represents the REDOR transform of the filter function $F(t)$.

We used this REDOR transform to determine the number of signals and to estimate the dipole–dipole couplings that govern the REDOR decays of the two peaks at 119 and 122 ppm. The REDOR transform derived by Mueller et al.¹⁵ was designed for the common case of two spin $S = I = 1/2$ (eq 9). We used the

(25) See, for instance: Harris, R. K. *NMR Spectroscopy*; Longman Scientific: Essex, 1986.

(26) Baumann, W.; Oprunenko, Y.; Günther, H. Z. *Naturforsch.* **1995**, *50a*, 429.

(27) Edlund, U. *Org. Magn. Reson.* **1979**, *12*, 661.

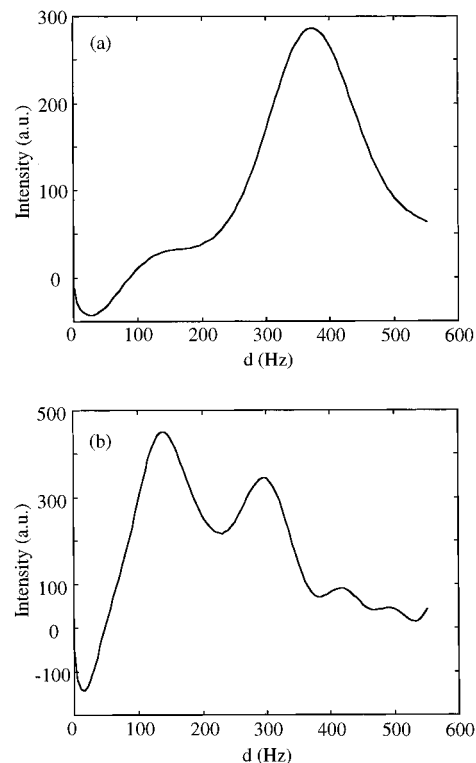


Figure 5. REDOR transformation of the decays of the peaks at (a) 78 ppm and (b) 119 ppm.

slightly revised kernel¹⁵

$$K(x) = \sqrt{2}x\{J_{-1/4}(x)Y_{1/4}(x) + J_{1/4}(x)Y_{-1/4}(x)\} - \sqrt{2}x^2\{J_{1/4}(x)Y_{3/4}(x) + J_{3/4}(x)Y_{1/4}(x) + J_{5/4}(x)Y_{-1/4}(x) + J_{-1/4}(x)Y_{5/4}(x)\} \quad (12b)$$

where

$$x = \zeta\sqrt{2}DN_C T_1/2\pi \quad (12c)$$

In eq 12c, $\zeta = 1$ if the refocussing π -pulses are applied on the $S = 1/2$ spins (eq 9), and $\zeta = 2$ if they are applied on the $I = 1$ spin (eq 8). Consequently, we used $\zeta = 2$. Due to the diverging kernel, the REDOR transform does not work very well on decays with small dipole–dipole couplings (in particular at high spinning speeds).¹⁵ Therefore, in order to suppress the centerband in eq 8, we subtracted 1/3 of the signal obtained without $\pi(^6\text{Li})$ -dephasing pulses from the signal obtained with $\pi(^6\text{Li})$ -dephasing pulses. This was made by first fitting an exponentially decaying function to the decay of the signal obtained without $\pi(^6\text{Li})$ -dephasing pulses and then subtracting 1/3 of this decay from the signal obtained with $\pi(^6\text{Li})$ -dephasing pulses. Since the diverging kernel also makes the REDOR transform rather sensitive to the noise level and baseline offset, we added an exponential decay to the Blackman–Harris filter used in ref 15.

In Figure 5, we show the dipole–coupling spectrum that occurs after a REDOR transformation of the decays of the ¹³C signals at 78 ppm (Figure 5a) and 119 ppm (Figure 5b). In Figure 5a only one peak occurs (as expected), the position of this peak is about 370 Hz. In Figure 5b, on the other hand, two peaks appear, which indicates that the ¹³C signal at 119 ppm is a superposition of two ¹³C signals (from two different carbons), that are located at different distances from the Li cation. The peaks in Figure 5b occur at about 130 and 300 Hz.

For the ¹³C signals at 114, 122, and 134 ppm, the REDOR transform yields single peaks at about 100, 140, and 300 Hz,

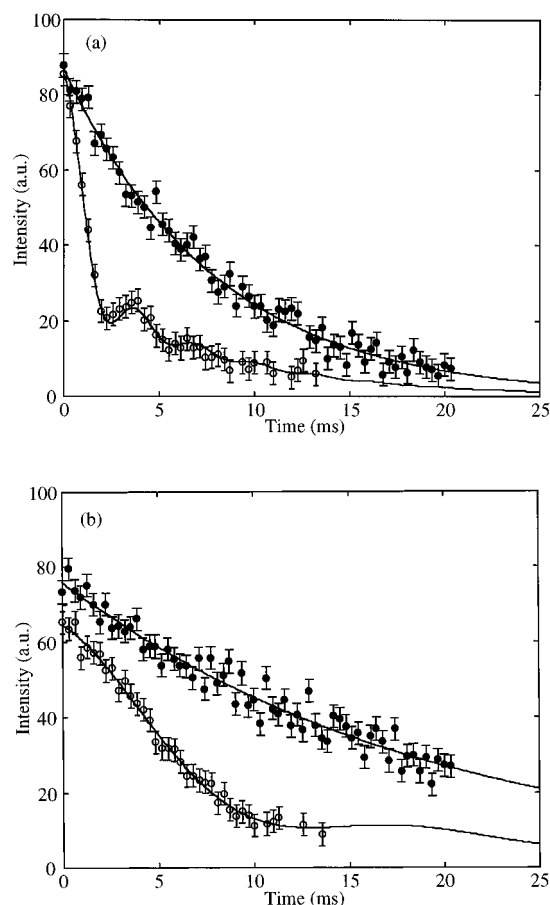


Figure 6. Best fits to the decays of the ^{13}C signals at (a) 78 ppm and (b) 114 ppm. The fitting procedure is described in the text, and the results from the best fit are listed in Table 1. For clarity, both sets of data are baseline corrected.

respectively. Since we believe that the ^{13}C signal at 122 ppm is a superposition, this indicates that the carbons contributing to this ^{13}C signal are located at about the same distance from the Li cation. We will return to this subject below. We had no problems with the diverging kernel as reported by others.²⁸

Calculation of D . In order to determine the distance between ^6Li and the three assigned ^{13}C in the fluorenyl complex, we must determine the corresponding dipole–dipole coupling (D) more accurately. This was made by a simultaneous nonlinear least-squares fit of eq 8 to the ^{13}C -decays obtained with and without π -pulses on the ^6Li resonance using the Levenberg–Marquardt routine.²⁴ (For the data set obtained without the π -pulses on ^6Li , we thus only fit the exponential decay in eq 8.) According to eq 8 there are three unknown parameters that determine the decay: the initial amplitude (S_0), the dipole–dipole coupling (D), and the transverse relaxation time T_2 . However, from a practical point of view we must add three new parameters, viz.: a constant baseline correction in eq 8, and a separate amplitude and baseline correction for the decay without refocussing π -pulses (since this decay was acquired with a slightly different number of accumulations, cf. the Experimental Section). In total there are thus six unknown parameters. Of these parameters, the approximate value of the two S_0 are known from the initial amplitude of the signals, and the REDOR transform gives an estimate of the dipole–dipole coupling.

In Figure 6 we show two examples of the best fits. In Figure 6a it is the decay of the peak at 78 ppm, and in Figure 6b it is the decay of the peak at 114 ppm. The resulting parameters from the best fit to the decays of the peaks at 78, 114, and 134

Table 1. Parameters Derived from a Fit of Eq 8 to the Decays of the Assigned ^{13}C Peaks

peak (ppm)	carbon	d^a (Hz)	T_2 (ms)	r_{IS} (Å)
78	9	354 ± 33	8 ± 1	2.32 ± 0.07
114	3	71 ± 12	19 ± 6	3.97 ± 0.22
134	9a	271 ± 54	15 ± 10	2.54 ± 0.17

^a $d = D/2\pi$, is the dipole–dipole coupling expressed in Hz. The uncertainties ($\pm 3\sigma$) represent propagated random noise from the spectra.

ppm are listed in Table 1. Notice that for the peak at 78 ppm (Figure 6a), where the dipole–dipole coupling is large, both decays are described by the same transverse relaxation time. This indicates that the set-up of the NMR spectrometer was good and that the weaker dipole–dipole couplings derived from the peaks at 114 and 134 ppm are not subject to systematic errors. As a second indication of the accuracy of the experiments, the calculated rms deviation of the fit to the experimental intensity equals the noise level in the ^{13}C spectra ($\sigma_{\text{noise}} \approx 3$ arbitrary units, au, cf. Figure 6), as expected.

Locating the Li Cation. To start with, we assume that the Li cation only occupies one site above the fluorenyl framework. (In the Appendix we discuss the effects of dynamics on the dipole–dipole coupling D .) Using eq 4 we calculate the distance r_{IS} between the ^6Li cation and the three assigned carbons of the fluorenyl framework. For the particular case of ^6Li and ^{13}C , eq 4 reduces to

$$r_{\text{IS}} = \sqrt[3]{\frac{\mu_0 \gamma_{^6\text{Li}} \gamma_{^{13}\text{C}} \hbar}{4\pi D}} \approx \sqrt[3]{\frac{4446 \text{ Hz}}{d}} 10^{-10} \text{ m} \quad (13a)$$

where

$$D = 2\pi d \quad (13b)$$

In Table 1 we list the distances r_{IS} derived in this manner. Notice that carbons 9 and 9a are relatively close to the Li cation, whereas carbon 3 is more distant. This implies that the Li cation is located somewhere close to the symmetry plane $x = 0$ (cf. Figure 4). This conclusion is supported by the symmetry of the ^{13}C spectrum of the fluorenyl system (cf. the Appendix), hence x_{Li} was set to zero in the coordinate system defined in Figure 4. There are thus two coordinates to determine, y_{Li} and z_{Li} , and three input data—the r_{IS} determined from the three assigned carbon peaks at 78, 114, and 134 ppm (cf. Table 1). In order to continue, the coordinates for the carbons of the fluorenyl framework are needed. Unfortunately, there is no X-ray structure determination of this system. In the following, we shall therefore assume that the coordinates of the carbons, of the fluorenyl framework, are similar to those in the PMDTA complex of fluorenylsodium,²⁹ which are listed in Table 2 and displayed in Figure 4. In this complex, the sodium cation is located above the central five-membered ring.

In the one-site model, the distance between the Li cation and each of the carbons is given by

$$R_{k,\text{IS}} = \sqrt{(x_{\text{Li}} - x_k)^2 + (y_{\text{Li}} - y_k)^2 + (z_{\text{Li}} - z_k)^2} \quad (14)$$

where the subscript k refer to the index of the carbons in Figure 4 and (x_k, y_k, z_k) are the coordinates for these carbons (cf. Table 2). In eq 14 the distances $R_{k,\text{IS}}$ are written in upper case to indicate that these parameters are adjustable and vary with $(x_{\text{Li}},$

(28) Rakovska, A.; d'Espinoose, J.-B.; Fretigny, C.; Legrand, A.-P. *13th European Experimental NMR Conference*; Paris, 19–24 May 1996.

(29) (a) Corbelin, S.; Kopf, J.; Weiss, E. *Chem Ber.* **1991**, *124*, 2417. (b) The symmetrization changes the carbon coordinates by about 0.01 Å or less.

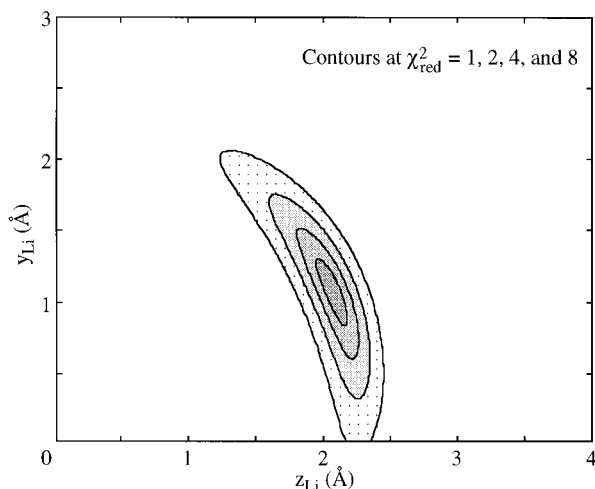


Figure 7. Contour plot of χ_{red}^2 in eq 15 vs the position of the Li cation in the yz -plane. The one-site model with $x_{\text{Li}} = 0$ is assumed. The contour levels are as indicated. The minimum $\chi_{\text{red}}^2 \approx 0.6$ is obtained at $y_{\text{Li}} = 1.07$ Å and $z_{\text{Li}} = 2.08$ Å.

y_{Li} , z_{Li}). To estimate the position of the Li cation we calculate the reduced “ χ -square”²⁴

$$\chi_{\text{red}}^2 = \frac{1}{4} \left[\left(\frac{R_{3,IS} - r_{3,IS}}{\sigma_{3,IS}} \right)^2 + \left(\frac{R_{9,IS} - r_{9,IS}}{\sigma_{9,IS}} \right)^2 + \left(\frac{R_{9a,IS} - r_{9a,IS}}{\sigma_{9a,IS}} \right)^2 \right] \quad (15)$$

which is expected to decrease to about unity—if the model describes the data properly, and the standard deviations ($\sigma_{k,IS}$, $k = 3, 9, 9a$) of the distances determined by the REDOR experiment ($r_{k,IS}$, $k = 3, 9, 9a$) are correctly estimated. (In eq 15, the factor 1/4 is determined by the number of degrees of freedom.) A contour plot of χ_{red}^2 vs y_{Li} and z_{Li} is shown in Figure 7, which reveals a minimum at $(x_{\text{Li}}, y_{\text{Li}}, z_{\text{Li}}) = (0, 1.07, 2.08)$ Å with $\chi_{\text{red}}^2 \approx 0.6$. This implies that the one-site model describes the experimental data and that the propagated uncertainties ($\sigma_{k,IS}$, $k = 3, 9, 9a$) are properly estimated.

From a least-squares fit, where y_{Li} and z_{Li} are varied, we obtain $y_{\text{Li}} = 1.1 \pm 0.2$ Å and $z_{\text{Li}} = 2.1 \pm 0.1$ Å, where the uncertainties correspond to $\pm 3\sigma$. As mentioned, this position of the Li cation above the five-membered central ring is also supported by a previous ⁷Li solid-state NMR investigation.^{4d}

We thus conclude that the one-site model for the Li cation appears to be correct; however, as discussed in the Appendix, exchange of the Li cation between several sites close (about 0.5 Å) to the position determined here will hardly shift the observed dipole–dipole couplings outside the range given by their uncertainties. A slightly mobile Li cation can thus account for the observed dipole–dipole couplings too. In such a case, the position of the Li cation determined with the one-site model above is approximately at the site that is closest to the fluorenyl complex (cf. the Appendix). As mentioned above, no dynamics of the fluorenyl framework could be detected in the range 213–273 K, whereas a dynamic process has been observed in the TMEDA ligand.^{4a} This dynamic process is most probably the same dynamic processes studied in detail with ¹³C, ¹⁵N, and ⁷Li solid-state NMR spectroscopy.²⁶ It thus appears as if this motion of the TMEDA ligand hardly influence the relative position of the Li⁺ ion and the fluorenyl complex.

Figure 8 displays a stereo drawing of the position of the Li⁺ ion with respect to the fluorenyl framework. The distances obtained here (cf. Table 2) are consistent with the corresponding distances found by X-ray in the TMEDA complex of indenyl-

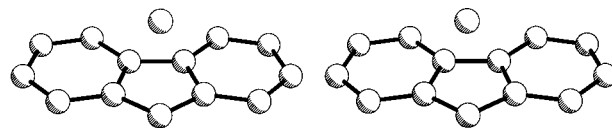


Figure 8. Stereoview of the determined structure of solid fluorenyllithium.

Table 2. Coordinates for the Carbons in the Fluorenyl Anion based on the PMDTA Complex of Fluorenylsodium²⁹ and the Calculated Distance between the Carbon and the Li Cation in the TMEDA Complex of Fluorenyllithium

carbon	x (Å)	y (Å)	z (Å)	$r_{k,\text{calc}}$ (Å)	δ , ppm ^a
9	0	0	0	2.34	78
9a	1.15	0.84	0	2.39	134
1	2.53	0.56	0	3.31	119
2	3.44	1.60	0	4.05	122
3	3.00	2.93	0	4.10	114
4	1.67	3.24	0	3.44	122
4a	0.71	2.22	0	2.48	119

^a List of the chemical shifts obtained from the assignment (see text).

lithium.³⁰ In this system the lithium cation is nearly symmetrically located over the five-membered ring. The distances in the fluorenyl complex is, however, somewhat longer. This discrepancy can be explained by a difference in the charge distribution in the two anions.

With the location of the Li cation determined we calculate the distance to the other carbons, $r_{k,\text{calc}}$; these are listed in Table 2. Comparison with the $r_{k,IS}$ in Table 1 shows that the results of the one-site model (Table 2) reproduce the experimental data. Furthermore, it is now possible to assign the peaks at 119 and 122 ppm. If we fit eq 8, but now as a superposition of two signals with different dipole–dipole couplings, to the decay of the superposition at 119 ppm, the best fit corresponds to two signals with amplitudes 110 and 80 au and with dipole–dipole couplings $d = 123 \pm 9$ and 291 ± 33 Hz, respectively. This corresponds to internuclear distances equal to 3.31 ± 0.08 and 2.48 ± 0.09 Å, respectively. According to Table 1, the peak at 119 ppm is thus a superposition of the signals from carbons 1 and 4a, respectively. This assignment of the peak at 119 ppm agree with the results from a selective polarization experiment,³¹ which showed that this peak is a superposition of at least two signals, one being from a nonprotonated carbon (i.e., carbon 4a). The same experiment also showed that the peak at 134 ppm is due to an other nonprotonated carbon (i.e., carbon 9a).

The superposition at 122 ppm should then correspond to carbons 2 and 4. According to Table 2, the distance between the Li cation and these carbons is about 3.4 and 4.0 Å, respectively. This corresponds to a dipole–dipole coupling of about 110 and 70 Hz. Since these values are relatively similar, the REDOR transform cannot resolve them, nor is it possible make a least-squares fit to the decay. However, if we perform the least-squares fit with the dipole–dipole couplings set to 70 and 110 Hz, we can reproduce the decay of the signal at 122 ppm. The best fit yields about equal intensity for the two signals. It can thus be concluded that the peak at 122 ppm is a super position of the signals from carbons 2 and 4. In Table 2, we list the assignment of the carbons in the fluorenyl framework.

To conclude, we have shown that the REDOR experiment is extremely useful for structural studies of solid organolithium compounds. It was possible to determine the position of the Li cation with respect to the anionic fluorenyl framework to

(30) Rhine, W. E.; Stucky, G. D. *J. Am. Chem. Soc.* **1975**, *97*, 737.

(31) Xiaoling, W.; Shanmin, Z.; Xuewen, W. *J. Magn. Reson.* **1988**, *77*, 343.

within $\pm 0.2 \text{ \AA}$ and show that a model with the Li cation in one site (located symmetrically with respect to the fluorenyl framework) readily describes the experimental results. Finally, with the REDOR transform supported with a least-squares fit, it was also possible to assign all peaks from the fluorenyl framework in the ^{13}C MAS spectrum.

Experimental Section

Sample Preparation. *n*-Hexane was distilled from sodium metal and TMEDA from LiAlH_4 . ^6Li (95–96%) enriched lithium metal was provided by Oak Ridge National Laboratory. ^6Li enriched *n*-butyllithium was prepared by the reaction of *n*-butyl chloride and enriched lithium metal in dry hexane under an argon atmosphere using ultrasonic treatment. The supernate was isolated by double syringe techniques. The concentration of the *n*-butyllithium was determined by titration with *N*-pivaloyl-*o*-toluidine.³² Fluorene was dissolved in dry *n*-hexane and 1 equiv of TMEDA, followed by the addition of 1.1 equiv of the ^6Li enriched *n*-butyllithium, at room temperature. A bright yellow solid was immediately formed. The solvent was removed, and the solid material was dried under vacuum. The sample was loaded in a special airtight Kel-F insert for a 7 mm Bruker MAS rotor in an argon filled drybox.

The REDOR Experiment. ^{13}C CP-MAS and REDOR spectra were acquired on a Bruker DSX 300, operating at 299.87 MHz for ^1H , 75.41 MHz for ^{13}C , and 44.13 MHz for ^6Li . The sample (about 100 mg) was packed in an air tight insert and spun in a 7 mm spinner at a rate of 6200 Hz. The experiment was executed in a pseudo-2D-fashion, with the sequence depicted in Figure 1b. Cross polarization was executed with 1 ms contact time with a proton ramp spin lock pulse to increase signal stability and assure Hartmann–Hahn match also for weaker proton-carbon dipolar couplings at this spin rate. A cw decoupling field of 100 kHz was used. Pulse lengths were 14 μs for the ^6Li and 13 μs for the ^{13}C π pulse. One hundred sixty scans were added per row in the comparison experiment with no $\pi(^6\text{Li})$ -dephasing pulses, whereas 208 scans for the REDOR experiment with $\pi(^6\text{Li})$ -dephasing pulses was used. A 4 s repetition rate was used. Within one experiment, the REDOR recoupling sequence was incremented from 0 to 126 rotor periods in steps of two rotor periods. Significant signal intensity was left in the reference experiment after 126 rotor periods. Since we have about 95–96% enrichment of ^6Li and only observe the naturally abundant ^{13}C nuclei, the REDOR dephasing observed is due to the interactions between ^6Li and ^{13}C in the same complex. Furthermore, the decay of the ^{13}C peaks in the REDOR experiment is essentially (about 95–96%) due to the interaction with ^6Li . The remaining fraction of the sample (with ^7Li in the complex) does not significantly contribute to the characteristic dephasing in the REDOR experiment.

Acknowledgment. The authors thanks Prof. Jacob Schaefer for the comments on our new derivation of the REDOR decay. We are also grateful to Prof. Karl T. Mueller for his kind help with the REDOR transform and to Prof. U. Edlund for comments on the manuscript. This work was supported by grants from the Swedish Natural Science Research Council (NFR).

Appendix

Here we investigate the effect of dynamics on the experimentally determined dipole–dipole coupling. The one-site model discussed in the main text is not always a realistic model. This is because the relevant NMR time scale is on the order of

the difference in the static interaction it modulates.²⁵ (Of course there is always some motion present, for clarity, here we discuss motions between sites spaced by more than the experimental resolution.) For the particular case of the REDOR experiment, a modulation in the dipole–dipole coupling D can be very slow and still be in the fast-exchange regime. This is because the critical time scale is determined by the inverse of the modulation in D , i.e., $1/\Delta D \geq 1/D$, which is on the order of milliseconds (cf. Table 1). For the present study, we can thus assume that all molecular motion that can reduce D will do this—since it is likely that the correlation times obey the inequality $\tau_{\text{fluct}} < 1/(5\Delta D)$.²⁵ In particular, if the symmetry of the fluorenyl complex is taken into account we should set $x_{\text{Li}} = 0$ in the one-site model.

In general, if the distance between a carbon and the Li cation (r_{IS}) fluctuates rapidly (i.e., faster than $1/\tau_{\text{fluct}} = 40\text{--}1000 \text{ s}^{-1}$ in our case), we will observe an average dipole–dipole coupling, which is the population weighted average over r_{IS} (cf. below). Under these conditions, the mean distance between the carbons and the Li cation is not given by eqs 4 and 13, rather we have

$$r_{\text{m}} \equiv \sqrt[3]{\frac{1}{\langle r_{\text{IS}}^{-3} \rangle}} = \sqrt[3]{\frac{\mu_0 \gamma_{^6\text{Li}} \gamma_{^{13}\text{C}} \hbar}{4\pi \langle D \rangle}} \quad (\text{A1})$$

where r_{m} is the mean distance defined by eq A1 and $\langle D \rangle$ is the mean dipole–dipole coupling determined by the REDOR experiment.

For example, if the Li cation occupy two sites above the fluorenyl framework and there is a rapid exchange ($\tau_{\text{exc}} < 1/(5\Delta D) \approx \text{ms}$) between these two sites, the REDOR experiment detects the mean distance r_{m} between these two sites and the carbons in the fluorenyl framework. Labeling the sites with A and B (populations P_{A} and $P_{\text{B}} = 1 - P_{\text{A}}$) the r^{-3} dependence of the dipole–dipole coupling yields with eq A1

$$\left(\frac{1}{r_{\text{k,m}}}\right)^3 = P_{\text{A}} \left(\frac{1}{r_{\text{k,A}}}\right)^3 + (1 - P_{\text{A}}) \left(\frac{1}{r_{\text{k,B}}}\right)^3 \quad (\text{A2})$$

where

$$r_{\text{k,A}} = \sqrt{(x_{\text{A,Li}} - x_{\text{k}})^2 + (y_{\text{A,Li}} - y_{\text{k}})^2 + (z_{\text{A,Li}} - z_{\text{k}})^2} \quad (\text{A3})$$

and $r_{\text{k,B}}$ expressed in a similar fashion. In eq A3, $(x_{\text{A,Li}}, y_{\text{A,Li}}, z_{\text{A,Li}})$ is the location of the A-site, whereas $(x_{\text{k}}, y_{\text{k}}, z_{\text{k}})$ is the coordinate for carbon k . In general there are thus seven unknown parameters for this simple two-site model (the coordinates and P_{A}).

Because of the r^{-3} dependence of the dipole–dipole coupling, $\langle D \rangle$ is essentially determined by the closest site. For example, if $P_{\text{A}} = P_{\text{B}} = 0.5$, $r_{\text{k,A}} = 2.0 \text{ \AA}$, and $r_{\text{k,B}} = 3.0 \text{ \AA}$ then eq A2 dictates that $r_{\text{k,m}} \approx 2.3 \text{ \AA}$, which is fairly close to $r_{\text{k,A}}$. To conclude, if there is a rapid exchange between several sites it is hard to observe the effects from the most distant sites if these are not heavily populated. With an increasing number of determined dipole–dipole couplings $\langle D \rangle$, it becomes easier to observe deviations from a one-site model. In favorable cases it may be possible to determine the location and population of more than one site.